



*Transactions, SMiRT-26*  
Berlin/Potsdam, Germany, July 10-15, 2022  
Division II

## **Leak Before Break Determination: Sensitivity of Analyst Input Parameter Choices**

**Jay Wallace<sup>1</sup>, Robert Tregoning<sup>2</sup>**

<sup>1</sup> Materials Engineer, US Nuclear Regulatory Commission, Washington, DC, USA

<sup>2</sup> Senior Technical Advisor, US Nuclear Regulatory Commission, Washington, DC, USA (Robert.tregoning@nrc.gov)

### **ABSTRACT**

A leak before break (LBB) benchmarking activity to compare international LBB evaluation practices and algorithms was performed under the auspices of Committee on the Safety of Nuclear Installations (OECD/NEA, 2021). Analysts from 11 participating countries were asked to perform an LBB analysis using well-defined benchmark parameters to better understand the practices within each country. Results from the benchmark showed that analysis approaches and assumptions to address factors that are not typically specified within countries' requirements can significantly impact LBB acceptability. This paper examines the sensitivity of the factors that were identified in the benchmark as important for LBB margins: material property selection; crack morphology parameters; crack face pressure (CFP); and weld residual stress. The evaluation illustrates the importance of sensitivity analyses when evaluating LBB acceptability, particularly on systems, such as the one studied in the benchmark, that are expected to have marginal LBB acceptability.

### **INTRODUCTION**

A leak before break (LBB) benchmarking activity has recently been performed under the auspices of CSNI. (OECD/NEA, 2021) The objective of this benchmark activity was to compare results from analyses among participating countries and to identify the effects of weld residual stress (WRS) and crack morphology. The benchmark problem inputs attempted to completely describe the conditions for an LBB evaluation to better understand the practices in the 11 countries that participated in the benchmark, and to compare the capabilities of the crack opening displacement (COD), critical crack size (CCS), and leak rate (LR) algorithms being employed. One unanticipated finding was that, within the narrowly defined parameter space of the benchmark description, the analyst's approach and assumptions strongly affected LBB acceptability. The parameters that most strongly affected the LBB margins were the material properties, crack morphology parameters, and consideration of crack face pressure (CFP) and WRS in COD estimates. These parameters were often not explicitly specified in countries' LBB requirements or approved analysis methods. Further information on the baseline study and countries' LBB requirements can be found in OECD/NEA (2021) and Tregoning et al. (2022). This paper investigates the sensitivity of LBB margins to these parameters using the U.S. Nuclear Regulatory Commission NUREG-0800 Standard Review Plan (SRP) 3.6.3 guidance.

### **PROBLEM DEFINITION**

The benchmark configuration consists of a 50.8 mm wide, square, Alloy 82 butt weld in a surge line pipe (outer diameter of 406.4 mm with a 40.462 mm wall thickness) containing a hypothetical through-wall circumferential crack located at the weld centerline. The base material on both sides of the weld is Type 304 stainless-steel, (Table 1) the operating temperature is 340°C and the detectable leak rate is specified to be 0.061 kg/s ( $\approx$  1 gpm). CFP is specified as 50% of the 15.5 MPa internal pressure. Normal operation (NO) and safe shutdown earthquake (SSE) loads are given in Table 2. COD-independent approximations of crack

This material is a work of the U.S. Government and is not subject to copyright protection in the United States. The views expressed herein are those of the authors and do not represent an official position of the US NRC.

morphology parameters for corrosion fatigue (CF) and primary water stress corrosion cracking (PWSCC) crack morphologies were also specified in the benchmark problem. (Table 3)

Table 1: Material Properties

Parameter	Strength Properties			Ramberg-Osgood Parameters			J-R Curve Parameters (Δa in mm)		
	E [GPa]	Sy [MPa]	Su [MPa]	σ <sub>0</sub> [MPa]	Alpha [-]	n [-]	J <sub>1c</sub> [kJ/m <sup>2</sup> ]	C1	C2
Weld	196.8	316.5	542.4	332.35	0.386	11.39	524.4	586.3	0.661
Base	176.7	153.6	443	200.9	15.64	3.75	1182	355.1	0.728

Equivalent material property values used in the present study were calculated as the weighted averages of mixtures of pipe and weld properties (Shim et al., 2011, Rudland et al., 2012) for the E, α, σ<sub>0</sub> and n terms in the Ramberg-Osgood (R-O) equation:

$$\varepsilon = \frac{\sigma}{E} + \alpha \frac{\sigma_0}{E} \left( \frac{\sigma}{\sigma_0} \right)^n \quad (1)$$

Table 2: NO and NO + SSE Loads

	Force from Pressure [kN]	Axial Force [kN]	Bending Moment [kN-m]
NO	1289.6	13.34	88.59
NO + SSE	1289.6	48.04	378.0

Table 3: Crack Morphology Parameters

Parameter	COD-Dependent Parameters (Rahman, 1995)				COD-Independent Parameters	
	CF	PWSCC	Air Fatigue	IGSCC	CF	PWSCC
μ <sub>L</sub> μm	8.8	16.9	6.5	4.7	40	114
μ <sub>G</sub> μm	40.5	113.9	33.65	80	40	114
η <sub>t(90)</sub> m <sup>-1</sup>	6730	5940	2008	28200	1730	5020
K <sub>G</sub>	1.02	1.01	1.05	1.07	1.1	1.2
K <sub>G+L</sub>	1.06	1.24	1.25	1.33	1.1	1.2

## ANALYSIS TOOLS

Analysis modules for COD (Young et al., 2016), LR (Kurth, Williams, 2016) and crack stability (Olson, Scott, Young, 2016) used in the current evaluation are from the Extremely Low Probability of Rupture project, xLPR. (US NRC, NUREG-2247, 2021) The COD module estimates elastic and plastic contributions to COD at the inside diameter (ID) and the outside diameter (OD) COD (ID-COD, OD-COD) using GE-EPRI-like influence functions for combined axial stress, CFP, and subsequent application of bending stress. (Young et al., 2013) CFP is assumed to be uniform through the wall thickness at 50% of the internal pressure.

The LR module, LEAPOR, (Williams, Yin, 2019) estimates the leak rate of a flashing subcooled liquid through a narrow crack using an empirically adjusted homogeneous equilibrium model that considers the two-phase mixture to be a pseudo-fluid. Crack morphology parameter inputs are internally converted to effective parameters based on the ratio of COD to global roughness, and these effective parameters are used in LR estimates.

Crack stability under NO + SSE loading was evaluated using an elastic-plastic J-estimation routine. (Brust, Gilles, 1994, Olson et al., 2016) The effects of CFP and WRS were not included in crack stability estimates.

Elastic WRS-induced COD changes were evaluated using a simple scheme developed along the lines of classical COD estimation schemes that use influence functions developed from finite element solutions. (Brust et al., 2000) The ID- and OD-COD contributions due to WRS were then added to the COD values determined by the COD module to determine the total COD.<sup>1</sup>

## RESULTS

LBB acceptance was based on the SRP 3.6.3 specifications which require that the leakage crack size (LCS) be determined for a LR that is 10 times the detectable LR. The LCS must be able to withstand 1.4 times the NO + SSE loads, and the CCS (i.e., the largest crack size that is stable under NO + SSE loading) must be at least twice the LCS to be acceptable. The SRP 3.6.3 load margin of 1.4 was not challenged for any combination of parameters evaluated here and is not considered further. For the configuration and loading studied, the CCS to LCS margin (CCS:LCS-margin) of 2.0 was marginally achieved for 10 times the specified 0.061 kg/s detectable LR when CF crack morphology (Table 3), 50% CFP and 100% weld material properties (Table 1) were used in the evaluation.

COD-independent CF and PWSCC morphology parameters (Table 3) were developed from COD-dependent values for benchmark participants who were not able to use COD-dependent parameters. The COD-independent values were developed to approximate the COD-dependent estimates for the benchmark weld joint configuration under the assigned NO loading, assuming 50% CFP and weld metal properties. Comparison of LCS estimates using COD-dependent and COD-independent parameters showed agreement for the two morphology descriptions within the range of the COD values evaluated in this study. (Figure 1a) Although only COD-dependent values are used in the present study, these results can be directly compared to the CSNI benchmark results. Note, however, that this good agreement is only the case for the particular geometries and loadings investigated; significant differences between COD-independent and COD-dependent results may occur for configurations where the ratio of the COD to the global surface roughness is different than that considered here.

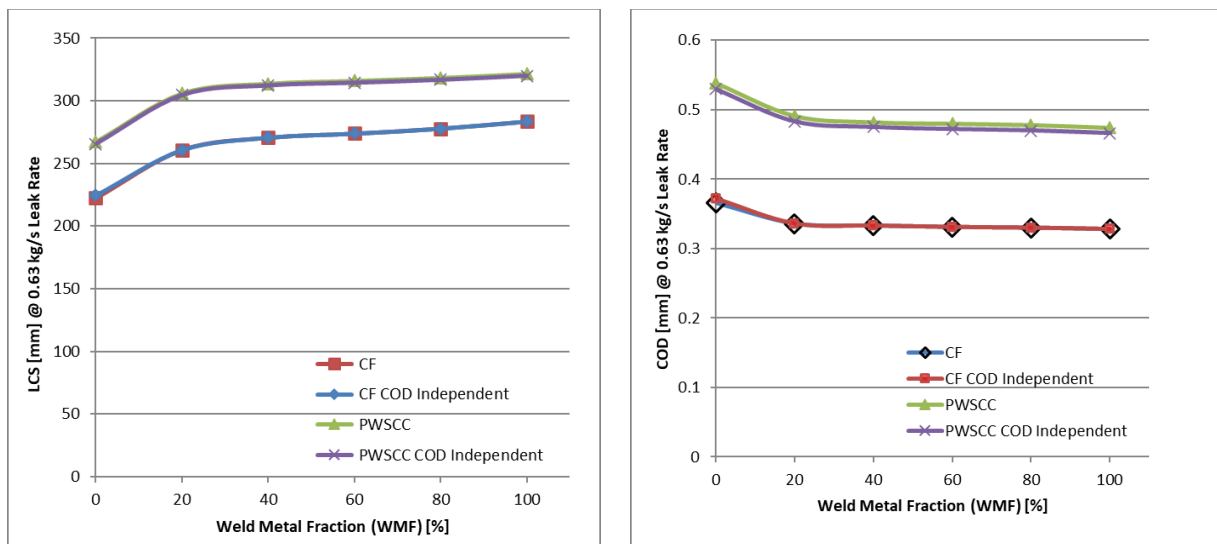


Figure 1: COD-dependent and COD-independent morphology effects a) LCS and b) mid-wall COD

<sup>1</sup> The authors acknowledge that summing elastic COD contribution from WRS and elastic-plastic contribution from external loading is a simplification

### Effective Material Mixture Property Sensitivity

(B)ase and (W)eld metal strength properties, (i.e., yield and ultimate strength, and Ramberg-Osgood (R-O) parameters) were provided for the benchmark problem but which material properties were to be used in the LBB analysis was not specified. Participants chose to use (B), (W) or a (M)ixture of (B) and (W) properties, and that choice had a significant effect on the LBB acceptability. (OECD/NEA 2021) The sensitivity of the choice of properties on the CCS:LCS-margin is investigated here.

Choice of material property is not simply the choice of a single bounding property, even when the crack is specified to be in a particular material. For a crack in a dissimilar metal weld, (DMW) the weld width and properties on either side of the weld are recognized as important contributors to the true crack-tip behavior. Shim et al. (2011) compared EPFM  $J$ -moment estimates for a circumferential crack in an Alloy 82 DMW between a ferritic steel nozzle and stainless-steel pipe to finite element modeling and found that the best agreement of the  $J$ -estimation scheme and finite element analysis resulted when a mixture of material properties on either side of the weld was used. The degree of agreement depended on the mixture properties used, with (B) properties giving the best agreement when the crack was near the base metal and (M) properties giving the best agreement when the crack was in the weld near the ferritic nozzle.

The benchmark problem material configuration, consisting of an Alloy 82 weld joining stainless-steel-piping on either side of the weld, is not the same as the DMW of the Shim study. The only possible mixture for the present configuration is that of stainless-steel (B) and Alloy 82 (W) materials. Therefore, the analyses here varied the weld metal fraction (WMF) from 0% (pure (B) properties) to 100% (pure (W) properties) and examined the effect on LCS and COD at the target leak rate.

The mid-wall COD for the LCS decreases significantly with increasing WMF from 0 to  $\approx 20\%$  and remains relatively constant with further WMF increase. (Figure 1b) Correspondingly, the LCS increases rapidly with WMF between 0 and  $\approx 20\%$  but then increases more slowly and in a relatively linear fashion with further WMF increase for the NO loading conditions and target LR used in this study. (Figure 2a) The coupled change in COD and LCS for fixed LR results from LR being related to crack opening area. The strong changes in COD and LCS as the mixture approaches (B) properties are likely related to increased (B) plastic behavior compared to that of (W) as the result of significantly lower R-O reference stress,  $\sigma_o$ , and exponent,  $n$ , parameters, in conjunction with the large R-O yield offset,  $\alpha$ , parameter.

WMF mixture properties were also used in CCS estimates. However, since the crack was assumed to propagate through weld metal, only weld metal J-R parameters were used in CCS estimates. WMF

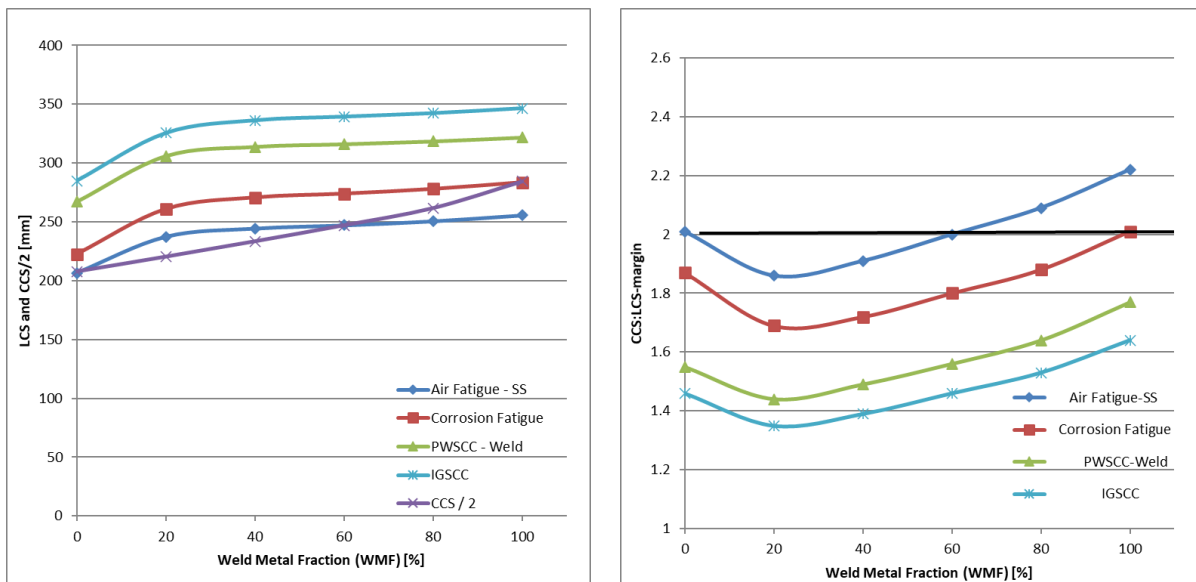


Fig 2: a) LCS and CCS / 2 and b) CCS:LCS-margin for a range of WMFs and crack morphologies

properties had a significant effect on CCS, with increasing WMF resulting in monotonic increase in CCS. (Figure 2a) Note that only LCS values below the CCS / 2 curve in Figure 2a would be acceptable for LBB.

The CCS:LCS-margin exhibits non-linear behavior with WMF, with a minimum at approximately 20% WMF. (Figure 2b) The CCS:LCS-margin sharply decreases with increasing WMF below 20% WMF as the result of an increase in LCS. (Figure 2a) Above 20% WMF where the LCS increase is minimal, the CCS:LCS-margin behavior is governed by the increasing CCS, and the CCS:LCS-margin increases. The CF morphology case that marginally met the LBB SRP 3.6.3 CCS:LCS-margin acceptance criterion of 2.0 when evaluated for 100% WMF is not acceptable for any of the property mixtures containing lesser WMF.

An additional calculation was performed to better understand the effect of plasticity and WMF on CCS:LCS-margin. The R-O yield offset term,  $\alpha$ , for the stainless-steel (B) material was set to a low value of 0.001 to approximate linear-elastic behavior. (Equation 1) Compared to the unmodified R-O value, this change for a WMF of 0% results in a decrease in COD of  $\approx 9\%$  for the target LR while the LCS and CCS increase by  $\approx 22\%$  and  $\approx 70\%$ , respectively, and the CCS:LCS-margin increases from 1.8 to 2.6. Increasing WMF above 20% increases the CCS:LCS-margin due to a similar change in effective material mixture properties.

### ***Crack Morphology Sensitivity***

SRP 3.6.3 requires that an LBB evaluation assumes a through-wall crack and evaluates whether the specified margins are met. However, despite being quite prescriptive for other analysis parameters, SRP 3.6.3 is notably silent on choice of the crack morphology to be used in the analysis. To evaluate the sensitivity of choice of crack morphology on LBB acceptability, a range of crack morphologies, from a low global roughness,  $\mu_G$ , air fatigue (AF) crack to a high  $\mu_G$  PWSCC crack, (Table 3) was investigated.

LBB acceptability for the present scenario is quite sensitive to the choice of crack morphology. AF crack morphology with its low roughness and low number of turns per length,  $\eta_{tL}$ , has a smaller LCS than any other crack morphology under similar conditions. (Figure 2a) Since CCS is not dependent on morphology, AF also has the largest CCS:LCS-margin, (Figure 2b) and could meet CCS:LCS-margin  $> 2$  acceptability with WMFs greater than approximately 60%. The other crack morphologies had CCS:LCS-margins that were generally  $< 2$  for all WMF values. Fluid flow through a crack is not dependent only on  $\mu_G$ . Despite having a relatively low  $\mu_G$  compared to that of PWSCC, cracks with IGSCC morphology exhibit low values of CCS:LCS-margin, apparently because the large  $\eta_{tL}$  term governs the IGSCC leak behavior and LCS.

Alloy 82/182 materials are subject to an active degradation mechanism, PWSCC, making PWSCC the most likely candidate for through-wall cracking in these weld materials. However, PWSCC crack morphology, with its relatively large  $\mu_G$  and  $\eta_{tL}$  values compared to AF or CF, requires significantly longer cracks to attain the target leak rate, resulting in low CCS:LCS-margin. This presents a conundrum for the analyst. Although a leaking crack in a DMW is more likely to be the result of PWSCC than CF or AF, selection of PWSCC crack morphology makes it difficult to meet LBB acceptance criteria, making selection of CF or AF morphology parameters a compelling choice for LBB analysis, particularly for smaller diameter piping which have an inherently smaller CCS:LCS-margin.

### ***Crack Face Pressure Sensitivity***

Incorporation of CFP in an LBB analysis is neither required nor prohibited by SRP 3.6.3. The benchmark problem specified that a CFP of 50% of the internal pressure be used in the analysis. However, CFP has not been incorporated in all COD tools, and there are questions about the realism of selecting a uniform 50% CFP over the entire wall thickness. This study evaluates the effect of CFP on COD and LCS for CF morphology using 3 different CFP fractions of the internal pressure, 0%, 50%, and 100%. While it is recognized that neither 0 or 100% CFP values nor the assumption of a uniform CFP through the pipe thickness is entirely realistic for through-wall cracks, these bounding values indicate the possible range of CFP effects.

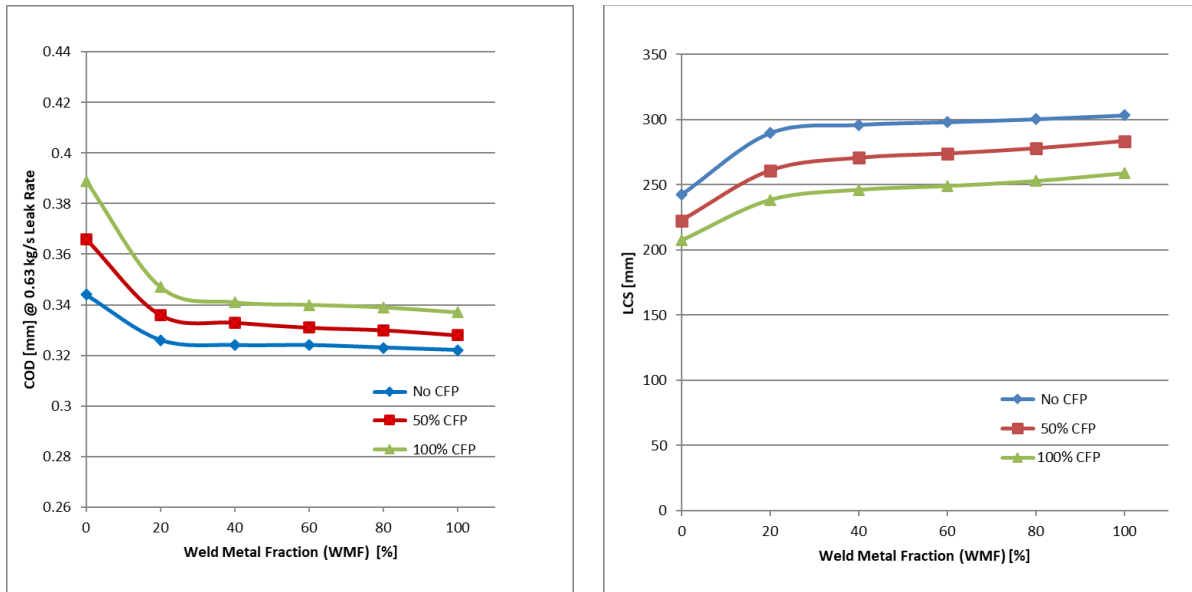


Figure 3: Effect of CFP on a) mid-wall COD and b) LCS

Incorporating CFP significantly affects COD (Figure 3a) and, subsequently, LCS. (Figure 3b) For the weld configuration, CF crack morphology and loading conditions here, inclusion of 100% CFP increased the COD at the target LR by nearly 15% for low WMF but significantly less for higher WMF. The change in COD with CFP is also reflected in change in LCS. (Figure 3b)

Because the magnitude of CFP stress is small relative to applied NO + SSE stresses, CFP is not expected to be a significant consideration in CCS estimation and has not been included here. As a result, the effects on the CCS:LCS-margin mirror those of the LCS; higher CFP promotes greater CCS:LCS-margins, making LBB acceptability more likely. (Figure 4)

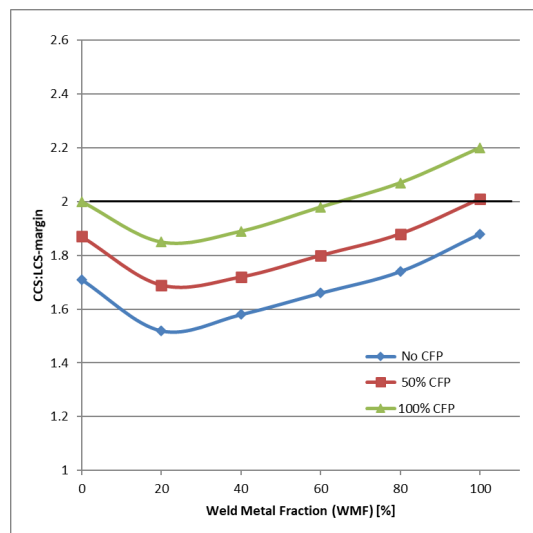


Figure 4: Effect of CFP on CCS:LCS-margin

Using a uniform through-thickness distribution of 50% of the internal pressure is an approximation, and a more representative through-wall pressure distribution is likely to change the results. Measurements of through-wall pressure profile of 2-phase leakage through relatively smooth artificial slits (Amos, 1984) have shown that the pressure profile is non-linear and strongly dependent of the degree of subcooling. It would also be expected that the pressure profile would be dependent on the COD :  $\mu_G$  ratio, as proposed for

the effective crack morphology determinations, somewhat further complicating CFP pressure distribution and LR analyses.

Initial efforts using finite element calculations to evaluate the effect of the CFP pressure profiles on COD (Twombly, 2020) compared COD from three different pressure profiles: a uniform 50% pressure profile, as is assumed here; a linear pressure profile decreasing from the ID to the OD; and a model, non-linear pressure profile from De Lorenzo (2017). The results show that significant changes in COD, thus LR, can result from different pressure profiles, particularly for long cracks. While more realistic, non-linear pressure profiles are not considered here, the results from this initial study are significant enough to suggest that incorporating of more realistic CFP models should be considered when evaluating systems with marginal LBB acceptability.

### Weld Residual Stress Sensitivity

As with CFP, consideration of WRS is neither required nor prohibited by SRP 3.6.3. Also, as with CFP, WRS is not expected to significantly affect the CCS, especially for the relatively ductile nickel-based alloy in this study. Therefore, the effect of WRS on COD, hence the LCS, is the focus of this evaluation. Two WRS distributions are considered: WRS-I profile (OECD/NEA, 2021) with a relatively flat compressive component over the inner half of the pipe wall and an increasing tensile component over the outer half of the wall; and WRS-II profile, a more complex profile determined by deep hole drilling measurements (US NRC, 2021) with a large compressive mid-wall component and tensile component over the outer portion of the pipe wall. (Equations 2 and 3, Figure 5a) Although WRS-II was not considered in the original benchmark study, inclusion here is to illustrate the magnitude of the effect that choice of WRS can have on LBB analysis.

The polynomial stress descriptions of these two profiles are given:

$$\text{WRS-I (in MPa)} = -101.3 - 167.58*(x/t) - 375.76*(x/t)^2 + 1165.75*(x/t)^3 \quad (2)$$

$$\text{WRS-II (in MPa)} = -254.3 + 4474.1*(x/t) - 23213.9*(x/t)^2 + 38329.9*(x/t)^3 - 19037.2*(x/t)^4 \quad (3)$$

where x is the distance from the inside wall and t is the wall thickness.

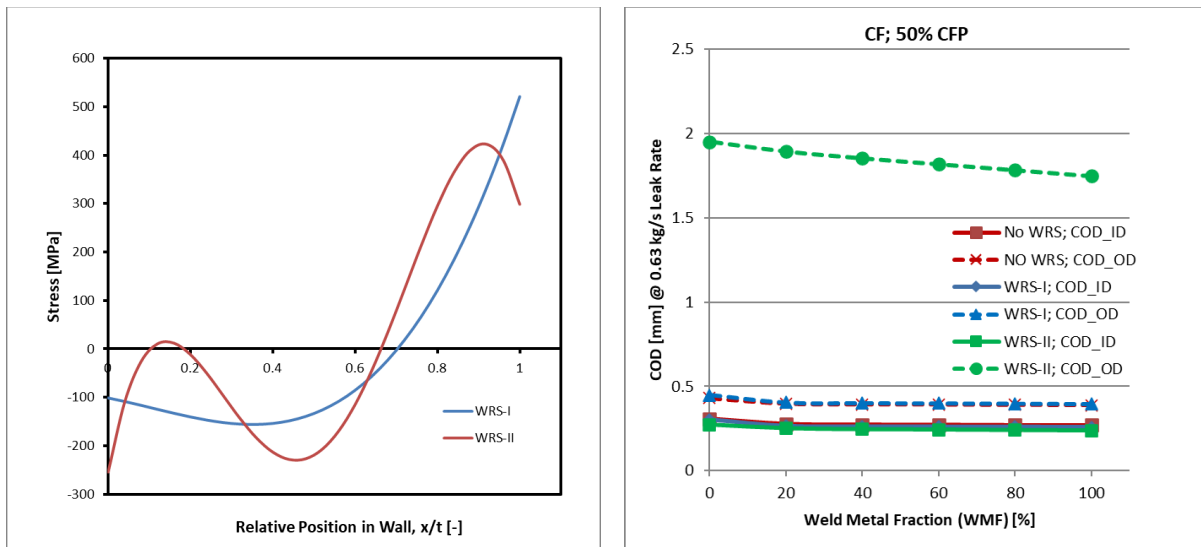


Figure 5: a) WRS distribution for WRS-I and WRS-II and b) ID- and OD-COD for the LCS

To evaluate the effect of WRS on CCS:LCS-margin, COD and LCS values were calculated for each WRS and compared to those determined previously without WRS. Inclusion of WRS-I was seen to have a minimal effect on either the ID- or OD-COD for the target leak rate for the CF morphology with 50% CFP. (Figure 5b) Since the application of WRS-I only minimally changed the ID- and OD-COD, the LCS is only minimally affected compared to the case without WRS. (Figure 6a)

The effect of WRS-II is far more dramatic. Application of the WRS-II stress profile to the ‘No WRS’ LCS results in complete closure of the crack at the ID, thus zero leakage; the crack needed to be lengthened significantly before the ID-COD opened and the target LR could be attained. (Figure 6a) Simultaneously, the OD-COD also increased significantly because of the increased crack length and the effect of WRS on OD-COD. (Figure 5b) The small decrease in ID-COD apparently dominates the LR behavior, at least for the small ID-COD here. While the trends in the results seem reasonable, it should be noted that the LR module exhibited issues in determining LR for the large differences in ID- and OD-COD that exist here.

Other processes that induce ID crack closure, such as a nearby closure weld, ID peening or weld overlay, while potentially beneficial for mitigating stress corrosion crack initiation and growth, would also be expected to have similar effects and tend to decrease the CCS:LCS-margin. As such, these factors should be included in a realistic LBB analysis.

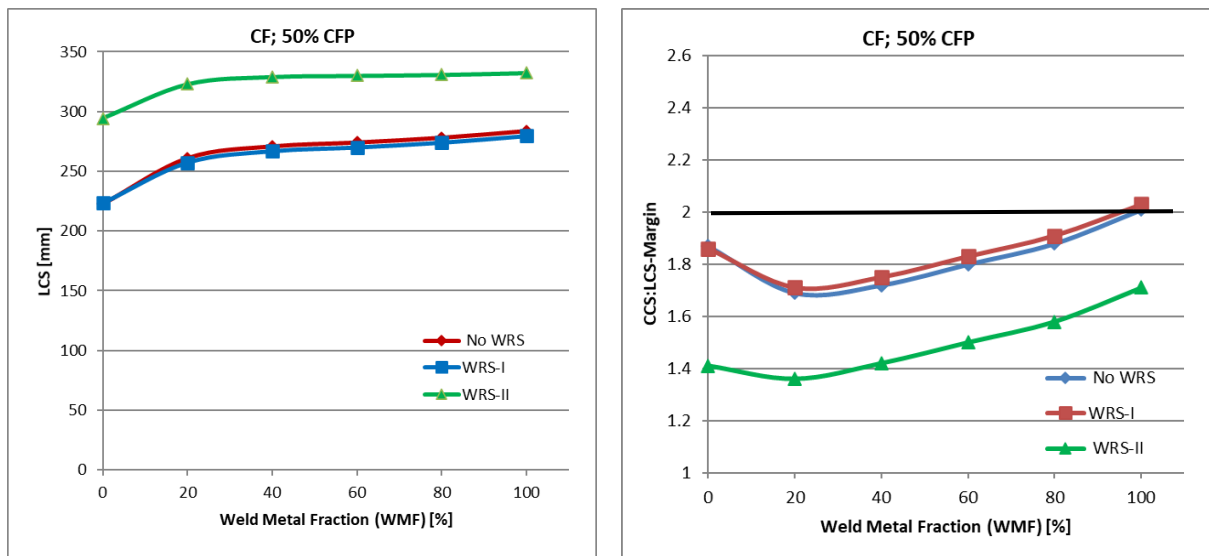


Figure 6: Effect of WRS choice on a) LCS and b) CCS:LCS-margin

### ***Bounding CCS:LCS-margin***

The contributions from the possible choices of mixture properties, crack morphology, CFP and WRS on the CCS:LCS-margin have been evaluated for the CSNI LBB-benchmark Alloy 82 weld in a surge line pipe. It has been shown that the individual parameters used in the LBB evaluation can result in either an increase or a decrease in the CCS:LCS-margin. Taking all the possible combinations of choices, bounding combinations can be determined. For the range of inputs evaluated here, the highest CCS:LCS-margin of 2.42 is found for 100% WMF, 100% CFP, AF crack morphology and either no WRS, or the WRS-I distribution. (Figure 7) Correspondingly, the lowest CCS:LCS-margin of 1.38 is found for 20% WMF with 0% CFP, PWSCC crack morphology and the WRS-II distribution. This wide range of CCS:LCS-margins, from 2.42 to 1.38, is particularly surprising because it solely results from selection of inputs and assumptions for a benchmark problem that was initially thought to be well-specified, suggesting that further guidance for evaluating LBB acceptability may be appropriate.



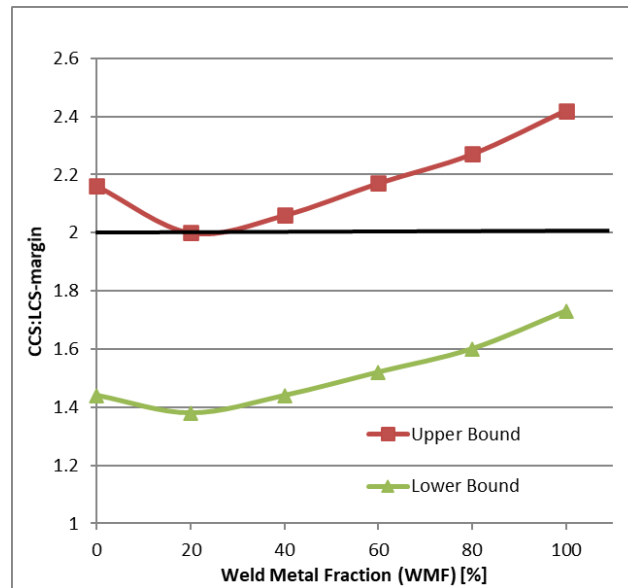


Figure 7: Bounding CCS:LCS-margin curves for the parameters investigated in this study

## SUMMARY

The LBB benchmark problem was developed with a configuration and loading that was marginally acceptable under nominally representative conditions. However, the current study demonstrates that the effect of just four parameters that are not specified in SRP 3.6.3 and are often unspecified in other countries' requirements, can affect the LBB margin by over 50%. Such uncertainty illustrates the importance of sensitivity analyses within an LBB evaluation to understand the effects on margin when evaluating acceptability. The appropriate use of sensitivity analysis and more realistic but validated models (e.g., CFP) are recommended if LBB is sought on systems, such as the one studied in the benchmark, that are expected to have marginal LBB acceptability.

## REFERENCES

- Amos, C., Schrock, V. (1984) "Two-Phase Critical Flow in Slits," *Nuclear Science and Engineering*, 88, 261-274
- Brust, F., Gilles, P. (1994) "Approximate Methods for Fracture Analysis of Tubular Members Subjected to Combined Tensile and Bending Loads," *ASME Journal of Offshore Mechanics and Arctic Engineering*, 1994;116:221
- Brust, F., Punch, E., Twombly, E. (2020) "Estimation Scheme for Weld Residual Stress Effect on Crack Opening Displacement," Technical Letter Report TLR-RES/DE/CIB-2021-01, <https://www.nrc.gov/docs/ML22124A002>
- DeLorenzo, M., Lafon, P., Seynhaeve, J.-M. and Bartosiewicz, Y., (2017) "Benchmark of Delayed Equilibrium Model (DEM) and Classic Two-phase Critical Flow Models Against Experimental Data," *International Journal of Multiphase Flow*, vol. 92, pp. 112-130
- Kurth, E., Williams, P. (2016) "xLPR Models Subgroup Report—Leak Rate, Version 1.1," <https://www.nrc.gov/docs/ML16341B047>
- OECD/NEA *Leak-Before-Break Benchmark Phase I Final Report* (2021). NEA/CSNI/R(2021)13, publication pending.
- Olson, R. (2016) "xLPR Models Subgroup Report—Crack Stability, Version 1.0, June 20, 2016," <https://www.nrc.gov/docs/ML16341B050>

- Olson, R., Kalyanam, S., Park, J.-S., Brust, F. (2016) "Improvement of the LBB.ENG2 Circumferential Through-Wall Crack J-Estimation Scheme," *Proceedings of the ASME 2016 Pressure Vessels and Piping Conference*, PVP2016-62264
- Rahman, S., Ghadiali, N., Paul, D., and Wilkowski, G. (1995) "Probabilistic Pipe Fracture Evaluations for Leak-Rate-Detection Applications," NUREG/CR-6004, U.S. Nuclear Regulatory Commission, doi:10.2172/50938
- Rudland, D., Lukes, R., Scott, P., Olson, R., Cox, A., Shim D.-J. (2012) "Dissimilar Metal Weld Pipe Fracture Testing: Analysis of Results and their Implications," *Proceedings of the ASME 2012 Pressure Vessels & Piping Conference*, PVP2012-78140
- Shim, D.-J., Wilkowski, G., Rudland, D. (2011) "Determination of the Elastic-Plastic Fracture Mechanics Z-factor for Alloy 182 Weld Metal Flaws," *International Journal of Pressure Vessels and Piping*, 88, p231-238
- Tregoning, R. et al. (2022) "CSNI Leak-Before-Break Benchmark – Summary of Phase I," *Structural Mechanics in Reactor Technology, SMiRT-26*, Berlin/Potsdam, Germany, July 10-15, 2022
- Twombly, E. (2020) "Effect of Crack Face Pressure Distribution on Crack Opening Displacements and Associated Leak Rates," Technical Letter Report TLR-RES/De/CIB-2021-01, <https://www.nrc.gov/docs/ML21077A051/>
- U.S. Nuclear Regulatory Commission (2007), *Standard Review Plan for the Review of Safety Analysis Reports for Nuclear Power Plants: LWR Edition — Design of Structures, Components, Equipment, and Systems, NUREG-0800, Leak-Before-Break Evaluation Procedures, Standard Review Plan 3.6.3, Revision 1.*, <https://www.nrc.gov/docs/ML0636/ML063600396.pdf>
- U.S. Nuclear Regulatory Commission (2020) "Weld Residual Stress Finite Element Analysis Validation Part II—Proposed Validation Procedure Final Report," NUREG-2228, <https://www.nrc.gov/docs/ML20212L592>
- U.S. Nuclear Regulatory Commission (2021) "Extremely Low Probability of Rupture Version 2 Probabilistic Fracture Mechanics Code," NUREG-2247, ADAMS Accession No. ML21225A736, <https://www.nrc.gov/docs/ML21225A736>
- Williams, P., Yin, S. (2013) "Prediction of the Leakage Rate for Cracked Pipes in Nuclear Power Plants," *Structural Mechanics in Reactor Technology Transactions, SMiRT-22*, San Francisco, California, USA - August 18-23, 2013
- Young, B., Olson, R., Scott, P. (2013) "Advances in COD Equations – Multiple Loading Modes: Concurrent Axial and Crack Face Pressure Loading with a Subsequent Applied Bending Moment," *Structural Mechanics in Reactor Technology Transactions, SMiRT-22*, San Francisco, California, USA - August 18-23, 2013
- Young, B., Benson, M., Scott, P., Olson, R. (2016) "xLPR Models Subgroup Report—Crack Opening Displacement, Version 1.0," ADAMS Accession No. ML16341B053, <https://www.nrc.gov/docs/ML16341B053>